

[Article]

Reconstructing the Tensor Model for the Reynolds Stress in Turbulent Channel Flow

TAKAHASHI Koichi

The tensor model for the Reynolds stress proposed in a previous work is reconstructed and applied to a turbulent channel flow. The qualitative feature of the experimental data are well reproduced.

That the Navier-Stokes equation is derivable from the variational principle without unholonomic condition was proved by Takahashi (2017), on which the dynamical effective viscosity model (DEVVM) was grounded. In addition to the kinematic viscosity, the DEVVM consists of mutually interacting complex scalar and vector fields that correspond respectively to the effective viscosity and the mean fluid velocity. When applied to channel and tube turbulent flows, the DEVVM gives quite simplified equations of motion and reproduces the experimental results for mean velocity (Takahashi 2017). In so far as these simplest turbulences are concerned, we may admit the conceptual success of the DEVVM.

Fluctuations of the velocity are another important quantities that specify the property of turbulence. The one researchers adopt as the indices of the velocity fluctuations is the Reynolds stress, $\overline{\delta u_i \delta u_j}$, where δu_i is a fluctuation of the velocity component u_i and the bar denotes ensemble average. Reynolds stress is a tensor. It is then natural to try to extend the DEVVM so as to incorporate a tensor, which we write R_{ij} . The first attempt of such an extension of DEVVM was done by Takahashi (2018a, 2018b), according to which, when applied to a channel turbulent flow, the tensor in the model exhibited behaviors that are consistent with the observed Reynolds stress at least in the central region. It should be noted that the tensor model in Takahashi (2018a, 2018b) does not alter the equations of motion for the effective viscosity and the mean velocity presented in Takahashi (2017).

However, in the above model, there were two shortcomings. First, the tensor was not symmetric and was not straightforwardly identified with the Reynolds stress. Second, the deviation of the model calculation for the symmetric components of the tensor from the experimental data was appreciably large near the wall.

We remedy the first deficit by rewriting the interaction Lagrangian, i.e., the terms that do not involve time derivative, in Takahashi (2018b) by replacing R_{ij} by

$$S_{ij} = (R_{ij} + R_{ji}) / 2 \quad (1)$$

or $R_i \equiv R_{ij}\sigma_j$ by

$$S_i = S_{ij}\sigma_j. \quad (2)$$

This replacement gives rise to the equations of motion for R_{ij} that is invariant under the exchange of i and j . Then the symmetry of the solution is assured if boundary or initial condition is symmetric. The equations (3.2a) ~ (3.2d) supplemented by (3.6) for S_{ij} in Takahashi (2018b) is nothing but the equation for R_{ij} . The relevant equations are recapitulated below.

$$\begin{aligned} ((\bar{\lambda} + \phi)R'_{xx})' - 2R_{xy}u'_x - \bar{g}_0\Sigma - \bar{g}_1R_{xx} - \bar{g}_4(\phi'^2 + u_x'^2) - \bar{g}_7\phi'^4 &= 0, \\ ((\bar{\lambda} + \phi)R'_{yy})' - \bar{g}_0\Sigma - \bar{g}_1R_{yy} - (\bar{g}_4 + \bar{g}_5)(\phi'^2 + u_x'^2) - (\bar{g}_6 + \bar{g}_7)\phi'^4 &= 0, \\ ((\bar{\lambda} + \phi)R'_{zz})' - \bar{g}_0\Sigma - \bar{g}_1R_{zz} - \bar{g}_4(\phi'^2 + u_x'^2) &= 0, \\ ((\bar{\lambda} + \phi)R'_{xy})' - R_{yy}u'_x - \bar{g}_1R_{xy} - \frac{1}{2}\bar{g}_2\tilde{f}_x\phi' - \frac{1}{2}(\bar{g}_3\phi + \bar{g}'_3)u'_x &= 0, \\ ((\bar{\lambda} + \phi)\Sigma')' - 2R_{xy}u'_x - (3\bar{g}_0 + \bar{g}_1)\Sigma - (3\bar{g}_4 + \bar{g}_5)(\phi'^2 + u_x'^2) - (\bar{g}_6 + 2\bar{g}_7)\phi'^4 &= 0. \end{aligned} \quad (3)$$

where $\Sigma = R_{xx} + R_{yy} + R_{zz}$. The prime denotes a differentiation with respect to y , where y is the ratio of the wall distance to the half channel width. ϕ and u_x are the appropriately normalized effective viscosity function and the mean velocity, which are known functions of y (Takahashi 2018a, 2018b). \bar{g}_0 represents the strength of coupling of R_{ij} to Σ , while \bar{g}_1 measures the strength of the self coupling. Then, the set of equations (3) uniquely determines the R_{ij} if boundary conditions are given. For the sake of simplicity, we restrict ourselves to the case of $\bar{g}_6 = 0$. From now on, we regard above R_{ij} as the Reynolds stress.

Concerning the second problem, we retry finding the best set of parameters by trial and error. The efficiency of this calculation may be somewhat raised if we notice the observed feature of the experimental data. For example, the experiment shows that the component R_{yy} of the Reynolds stress as a function of the distance from the wall has an extremum at $y = y_a \approx 0.25$ (Nishino & Kasagi 1990). Furthermore, by the symmetry of the experimental setup, R_{yy} should have another extremum at $y=1$. Thus we have

$$\int_{y_a}^1 ((\bar{\lambda} + \phi)R'_{yy})' dy = 0 \quad (4)$$

The equation of motion for R_{yy} tells that the integrand of (4) is expressed in terms of the model

parameters and R_{ji} . The latter are experimentally known. Then the equation (4) gives a constraint on the model parameters.

Calculations were performed with two sets of parameters and the result are shown in Fig. 1 and 2. The gross experimental feature of the Reynolds stress is reproduced well by the present calculations. In particular, the near-wall behavior of Σ due to the present calculation shows a remarkable improvement over the previous calculation given by Takahashi (2018b).

The result for the off-diagonal component R_{xy} is also shown in Fig. 1. Compare this with Fig. 1 in Takahashi (2018). We see that the agreement with the experiment is also remarkable ; the present recalculation does not spoil the preferable feature of the previous result.

In order to see the effect of some interaction terms, we repeat the calculation by varying model

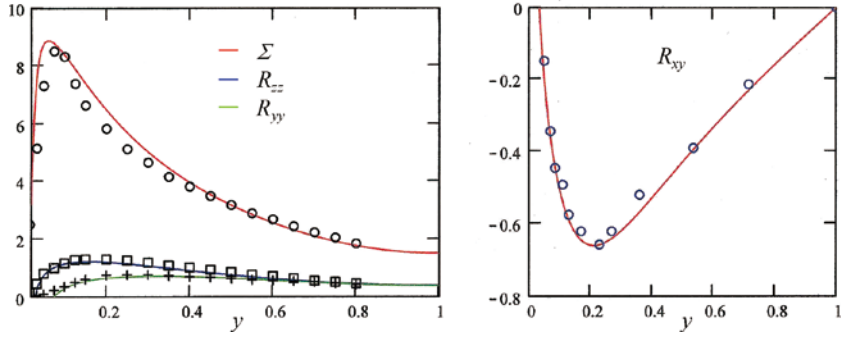


Fig. 1. Diagonal (left panel) and off-diagonal (right panel) components of R_{ij} calculated from (3). Red (top) curve : Σ . Blue (middle) curve : R_{zz} . Purple (bottom) curve : R_{yy} . Parameters are $\bar{g}_0 = -5.8$, $\bar{g}_1 = 66$, $\bar{g}_2 \tilde{f}_x = -63$, $\bar{g}_3 = -40$, $\bar{g}_3 = 40$, $\bar{g}_4 = -0.9$, $\bar{g}_5 = -0.9$, $\bar{g}_6 = -17$, $\bar{g}_7 = 34$, $\bar{\lambda} = 5.2$. Boundary values at $y=1$ are $R_{yy} = 0.38$, $R_{zz} = 0.4$, $\Sigma = 1.5$, $R'_{zz} = R'_{yy} = \Sigma' = 0$, $R_{xy} = 0$, $R'_{xy} = 0.78$. Symbols in the left panel denote the data of $Re_c = 3755$ for $\overline{\delta u^2}$ (circles), $\overline{\delta u_z^2}$ (squares) and $\overline{\delta u_y^2}$ (crosses) adapted from Nishino & Kasagi (1990). Circles in right panel denote the data of $Re_c = 2970$ for $\overline{\delta u_x \delta u_y}$ adapted from Wei & Willmarth (1987).

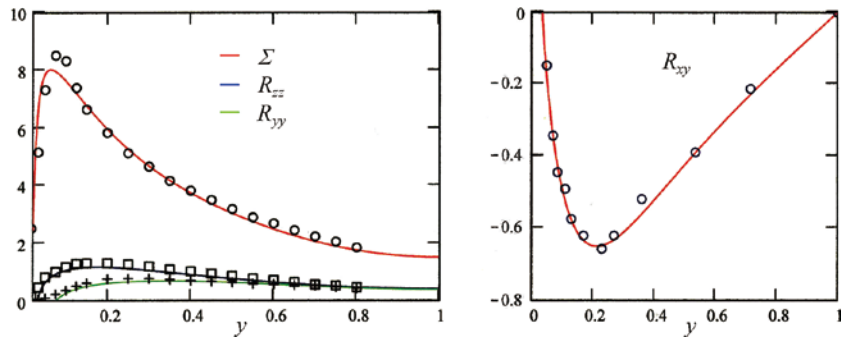


Fig. 2. Same as Fig. 1 with the same parameters and boundary values except $\bar{g}_0 = -6.1$.

parameters. One example of the result is shown in Fig. 2. There, only the value of \bar{g}_0 is changed to -6.1 , thereby the peaks of Σ , R_{yy} and R_{zz} are slightly decreased. R_{xy} , whose shape is very sensitive to $\bar{g}_2 \tilde{f}_x = -63$, remains unchanged.

That a restricted number of interaction terms reproduce the experimental data at least qualitatively is not a trivial fact because the functions φ , ∇u_x , R_{ij} and their higher derivatives do not form a complete set for continuous functions. Our result indicates that the invariant variational principle will constitute an essential ingredient in fluid dynamics.

References

- Takahashi K 2017, Mean-field theory of turbulence from variational principle and its application to the rotation of a thin fluid disk, *Prog. Theor. Exp. Phys.* 083J01.
- Takahashi K 2018a, Variational principle in hydrodynamics and mean-field theory of turbulence — A sequel of the paradox of vortices — II. Variational principle and mean-field theory of turbulence *Lib. Arts Rev. (Tohoku Gakuin Univ.)* No. 180 Jul., 29–72 (in Japanese).
- Takahashi K 2018b, Incorporating a tensor in the effective viscosity model of turbulence and the Reynolds stress *AIMS Mathematics* **3**(4), 554–564.
- Nishino K and Kasagi N 1990, Turbulence statistics measurement in a two-dimensional turbulent channel flow with the aid of the three-dimensional particle tracking velocimeter *Ronbunshyu B (Japan Soc. Mech. Eng.)* **56**, 116–125.
- Wei T and Willmarth W W 1989, Reynolds-number effects on the structure of a turbulent channel flow *J. Fluid Mech.* **204**, 57–95.